Journal of Materials Chemistry

Cite this: J. Mater. Chem., 2012, 22, 23175

www.rsc.org/materials

PAPER

Temporal stability of blue phosphorescent organic light-emitting diodes affected by thermal annealing of emitting layers†

Thomas Y.-H. Lee,[a] Qiang Wang,[a] Jason U. Wallace[b] and Shaw H. Chen*[ac]

Received 29th July 2012, Accepted 17th September 2012
DOI: 10.1039/c2jm35050e

Emitting layers were thermally annealed at 20 to 100 °C for varying durations without causing phase transformation in the rest of the PhOLEDs. Heating EMLs above their T_gs with a free surface created pinholes filled by the underlying TAPC melt with concurrent interlayer mixing to emit satellite peaks accompanying **FIrpic's** phosphorescence. With a robust glassy TmPyPB layer on top of the EML, pinholes and fortuitous fluorescence could be prevented. Annealing of **mCP:SiPh4:FIrpic** induced crystallization in 1 h, while **mCP-*o*-PhSiPh3:FIrpic** consistently resisted crystallization under all conditions. Crystallization or pinhole formation diminished EQE and driving voltage at the same time. Without incurring pinhole formation in the absence of a free surface presented by the EML, annealing of **mCP:SiPh4:FIrpic** at 60 °C for 1 h led to about 50% loss in EQE. In contrast, the pristine device's EQE persisted with **mCP-*o*-PhSiPh3:FIrpic** annealed at 60 °C for up to 24 h, beyond which other sources of device failure took over. The concept of bipolar hybrids holds promise for mitigating morphological instability as part of the challenge to the PhOLED device lifetime.

Introduction

Blue phosphorescent organic light-emitting diodes, PhOLEDs, are essential to full-color displays and solid-state lighting. The development of highly efficient and long-lived devices has remained a major challenge. In addition to the need for efficient and stable blue emitters,[1,2] the technological advances in blue PhOLEDs entail the understanding of intricate materials and interface degradation mechanisms that are electrochemical, photochemical (*i.e.* bond dissociation at excited states), thermal and morphological in nature.[3–5] Since the phosphorescent dopant is preferably dispersed at the molecular level into a host to prevent concentration quenching,[6] host materials with sufficiently high triplet energies, E_T, are imperative to blue emitters for excitons to remain on dopant molecules. Most of the existing host materials are capable of preferentially transporting holes[7,8] or electrons.[9–11] In consequence, charge recombination tends to occur near the interface of the emitting layer, EML, with either the electron- or hole-transport layer, which is detrimental to device efficiency and lifetime due to triplet–triplet annihilation[12] and triplet-polaron quenching[13] at high current densities pertaining to practical applications.

The capability of bipolar charge transport, physically mixed hosts[14–16] and hybrid hosts[17,18] with chemically bonded hole- and electron-transport moieties, HTMs and ETMs, has been demonstrated for broadening the recombination zone to alleviate efficiency roll-off. Although crystallization in the EML has been recognized as a factor limiting the device efficiency and lifetime,[19,20] there has been no definitive report using a polycrystalline EML relative to its amorphous counterpart of the same chemical composition without altering the other aspects of the OLED. Having been demonstrated for superior morphological stability against crystallization, bipolar hybrid compounds with flexible linkages[21] appear to be well suited for such an endeavor. Possessing sufficiently high E_T and hole mobility values, carbazole derivatives are the most commonly used HTMs for the construction of bipolar hybrid hosts.[22,23] Thanks to their ultra-high E_T values, arylsilane derivatives have been utilized as ETMs in blue PhOLEDs.[24,25] In the present study, **mCP** and **SiPh4** – the HTM and ETM, respectively – are linked with a propylene spacer to generate a new bipolar hybrid host, **mCP-*o*-PhSiPh3**, expected to have significantly improved morphological stability against crystallization over the physically mixed counterpart at the same HTM : ETM molar ratio. Through selective annealing of the EMLs comprising these two distinct hosts doped with **FIrpic**, the effects of thermally activated crystallization on blue PhOLED device performance will be elucidated in terms of external quantum efficiency and driving voltage.

Results and discussion

Depicted in Chart 1 are the molecular structures of the three compounds used in this study: **mCP**, **SiPh4** and

[a]*Department of Chemical Engineering, University of Rochester, Rochester, NY, 14627, USA. E-mail: shch@lle.rochester.edu*
[b]*Department of Mathematics and Natural Sciences, D'Youville College, Buffalo, NY 14201, USA*
[c]*Laboratory for Laser Energetics, University of Rochester, Rochester, NY, 14623, USA*
† Electronic supplementary information (ESI) available. See DOI: 10.1039/c2jm35050e

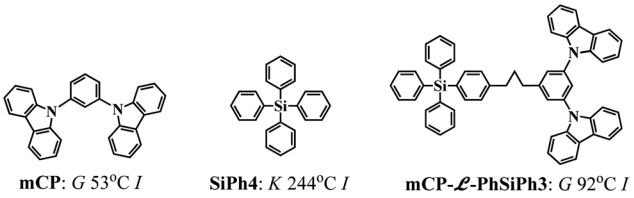

mCP: *G* 53°C *I* **SiPh4**: *K* 244°C *I* **mCP-*p*-PhSiPh3**: *G* 92°C *I*

Chart 1 Molecular structures of host materials with their thermal transition temperatures determined by DSC second heating scans. Symbols: *G*, glassy; *K*, crystalline; and *I*, isotropic.

mCP-*p*-PhSiPh3, accompanied by their thermal transition temperatures. The E_T values of **mCP**,[26] **SiPh4** (ref. 27) and **mCP-*p*-PhSiPh3** are 3.0, 3.5 and 3.0 eV, respectively, all sufficiently high for hosting **FIrpic**[28] (E_T = 2.6 eV) as the blue phosphorescent dopant; see Fig. S1† for the phosphorescence spectrum of a vacuum-sublimed **mCP-*p*-PhSiPh3** film. Thermogravimetric analysis was conducted to characterize the thermal stability of **mCP**, **mCP-*p*-PhSiPh3** and **FIrpic** up to 312, 383, and 378 °C, respectively (Fig. S2†), while that of **SiPh4** was reported previously at 482 °C.[29] According to the second heating scan using differential scanning calorimetry, DSC (Fig. S3†), glass transition temperatures, T_gs, were observed at 92 and 53 °C for **mCP-*p*-PhSiPh3** and **mCP**, respectively, while **SiPh4** is crystalline without detectable glass transition as observed under hot-stage polarizing optical microscopy.

To explore the effects of thermal annealing of EMLs on device performance, a series of PhOLEDs – ITO/MoO_3(3 nm)/TAPC(30 nm)/Host:**FIrpic**(10 wt%, 30 nm)/TmPyPB(10 nm)/BPhen(30 nm)/LiF(1 nm)/Al(100 nm) – were prepared comprising initially amorphous EMLs thermally annealed for predetermined durations. The layers underlying EMLs, ITO/MoO_3/TAPC, were found to remain amorphous with thermal annealing at 20 °C for up to 72 h and at 100 °C for 1 h, as evidenced by electron diffraction; see the inset in Fig. 1a. In addition, MoO_3 and Al layers were deposited on the annealed ITO/MoO_3/TAPC layers to fabricate hole-only devices, ITO/MoO_3(3 nm)/TAPC(30 nm)/MoO_3(3 nm)/Al(100 nm). The MoO_3 layer adjacent to ITO serves as a hole injection layer, while the other MoO_3 layer next to Al prevents electrons from being injected into the TAPC layer. The identical *I*–*V* curves to those prior to thermal annealing, as shown in Fig. 1a, indicate that hole injection and transport from ITO through TAPC was not affected by thermal annealing under all conditions without possible adverse effects caused by material and/or interface degradation in the absence of crystallization in any layer. The absence of pinholes in the TAPC layer under 100 °C annealing for 1 h was confirmed with the consistent, marginally higher current at the same driving voltage from 0 to 8 V without the 3 nm thick electron-blocking MoO_3 layer (Fig. 1b). In view of TAPC having a crystalline melting point at 183 °C,[30] the maximum crystallization rate from its melt is estimated at (183 + 273) × 0.90 − 273 = 137 °C.[31,32] Therefore, crystallization of the TAPC melt at 80 °C is expected to be slower than that at 100 °C since both thermal annealing temperatures are on the rising side of the bell-shaped crystallization rate profile. This observation assures that the results presented in Fig. 1 are applicable to annealing at 80 °C.

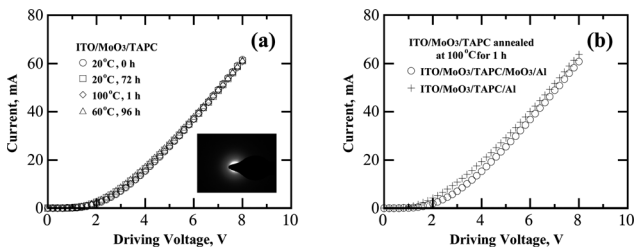

Fig. 1 Current as a function of driving voltage for hole-only devices upon thermal annealing of TAPC layers with a free surface at (a) 20 °C for 0 and 72 h, 100 °C for 1 h, and 60 °C for 96 h before completing the device, ITO/MoO_3(3 nm)/TAPC(30 nm)/MoO_3(3 nm)/Al(100 nm), and (b) 100 °C for 1 h before completing the device, ITO/MoO_3(3 nm)/TAPC(30 nm)/MoO_3(3 nm)/Al(100 nm) and ITO/MoO_3(3 nm)/TAPC(30 nm)/Al(100 nm). Inset in (a): electron diffraction image of the two-layer film, MoO_3(3 nm)/TAPC(30 nm), annealed with a free surface at 20 °C for 72 h and at 100 °C for 1 h in a glove box filled with nitrogen.

A mixed host, **mCP:SiPh4** at a 1 : 1 molar ratio, and a hybrid host, **mCP-*p*-PhSiPh3**, both doped with **FIrpic** at 10 wt%, constitute the EMLs for a legitimate comparison, other elements of the PhOLEDs being identical. For hole and electron injection layers, MoO_3 and LiF were used, respectively. The TAPC layer was deposited on the MoO_3 layer to aid in hole transport. Inserted between EML and LiF, BPhen serves not only as an electron-transport layer but also prevents exciton quenching by lithium ions diffusing into the EML.[33] The hole-blocking TmPyPB (E_T = 2.8 eV)[34] layer and hole-transporting TAPC (E_T = 2.9 eV)[35] layer should help to confine excitons on **FIrpic** in EML. Half-devices ITO/MoO_3/TAPC/EML were annealed at 20 °C for up to 72 h, and at 80 and 100 °C for 1 h under nitrogen before depositing TmPyPB/BPhen/LiF/Al sequentially to complete PhOLED devices. While the BPhen film with a free surface was found to crystallize at 20 °C overnight, the three freshly deposited layers on top of the EML, TmPyPB(10 nm)/BPhen(30 nm)/LiF(1 nm), were verified to be amorphous with polarizing optical microscopy and electron diffraction (see Fig. S4†). As shown in Fig. 2, crystallization was observed under polarizing optical microscopy in the EML comprising **mCP:SiPh4:FIrpic** annealed at 20 °C for 24 to 72 h and at 80 and 100 °C for 1 h, while the EML comprising **mCP-*p*-PhSiPh3:FIrpic** remained amorphous under the same annealing conditions. The amorphous character of the pristine **mCP:SiPh4:FIrpic** and that of **mCP-*p*-PhSiPh3:FIrpic** annealed at 20 °C for up to 72 h and 80 and 100 °C for 1 h were further validated by electron diffraction; see the inset in Fig. 2a. The morphological stability of **mCP-*p*-PhSiPh3:FIrpic** against crystallization over that of **mCP:SiPh4:FIrpic** is imparted largely by the flexible linkage in the former.[21]

Degradation of materials or interfaces could be inevitable in operational devices during characterization over a range of current density up to 50 mA cm^{-2}. Potential electrochemical, morphological, photochemical, and thermal degradations must be precluded to enable the effects of crystallization in EMLs to be scrutinized. *Pristine PhOLEDs* referred to hereafter represent untested devices consisting of all amorphous layers except EMLs independently characterized as amorphous or polycrystalline upon thermal annealing. As indicated by symbols + and × in Fig. 3, cumulative characterizations of devices consisting of

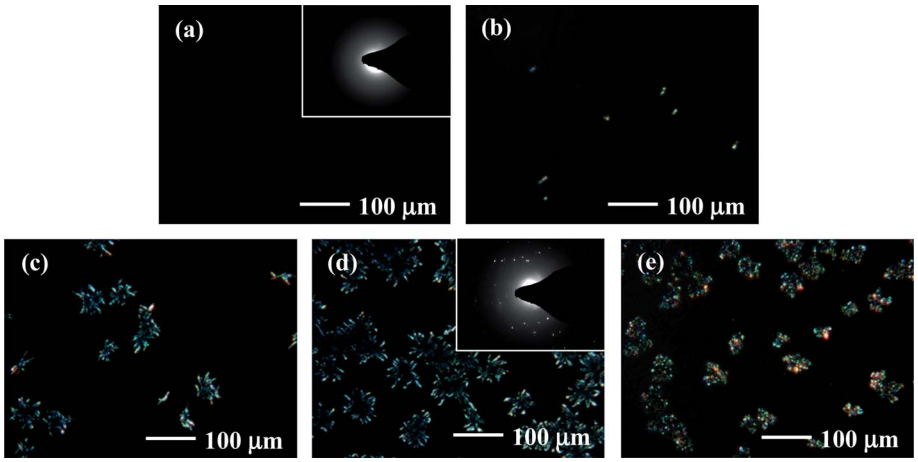

Fig. 2 Polarizing optical micrographs of ITO/MoO_3/TAPC/**mCP:SiPh4:FIrpic** kept at the ambient temperature of 20 °C for (a) 0 h, (b) 24 h, (c) 48 h, (d) 72 h, and (e) 80 and 100 °C for 1 h. Inset in (a): electron diffraction image of MoO_3/TAPC/**mCP:SiPh4:FIrpic** prior to thermal annealing; inset in (d): electron diffraction image of MoO_3/TAPC/**mCP:SiPh4:FIrpic** annealed at 20 °C for 72 h with calculated *d*-spacings[36] ranging from 0.14 to 0.47 nm; (a) with inset also serves to represent the amorphous character of MoO_3/TAPC/**mCP-*S*-PhSiPh3:FIrpic** annealed with a free surface at 20 °C for up to 72 h, and at 80 and 100 °C for 1 h each in a glove box filled with nitrogen.

mCP-*S*-PhSiPh3:FIrpic and **mCP:SiPh4:FIrpic** exhibit the same driving voltages and external quantum efficiencies, EQEs, as those of pristine PhOLEDs at 10 and 50 mA cm^{-2}, thus precluding potential adverse effects caused by repeated current drives incurred with device characterization. All PhOLEDs with both types of the EML annealed at 20 °C for up to 72 h and with **mCP-*S*-PhSiPh3:FIrpic** at 80 °C for 1 h exhibit nearly the same phosphorescence spectra as **FIrpic** at 10^{-5} M in chloroform.[28] Compared to **mCP-*S*-PhSiPh3:FIrpic**, polycrystallinity is present in **mCP:SiPh4:FIrpic** upon thermal annealing of ITO/MoO_3/TAPC/EML at 20 °C for 24 through 72 h and at 80 and 100 °C for 1 h (Fig. 2b–e *versus* Fig. 2a).

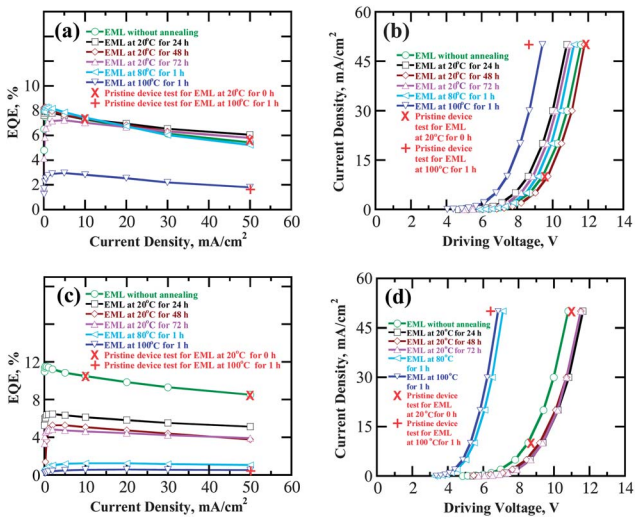

Fig. 3 (a) EQE and (b) driving voltage as functions of current density for PhOLED devices containing **mCP-*S*-PhSiPh3:FIrpic**, and (c) EQE and (d) driving voltage as functions of current density for PhOLED devices containing **mCP:SiPh4:FIrpic** with half-devices, ITO/MoO_3/TAPC/EML, annealed at 20 °C for up to 72 h and at 80 and 100 °C for 1 h. Typical experimental errors for EQE and driving voltage are ±10 and ±8%, respectively, of the mean from three separate devices. Pristine PhOLED devices were characterized at 10 and 50 mA cm^{-2} with pristine EMLs (×), and at 50 mA cm^{-2} with half-devices up to EML annealed at 100 °C for 1 h (+).

Annealing of EMLs above the mixed and hybrid hosts' T_gs at 57 and 97 °C (Fig. S3c and d†), respectively, produced satellites at about 420 and 580 nm (Fig. S5a and b†) flanking **FIrpic's** emission peaks at 470 and 500 nm. These fortuitous satellites are identifiable with emission from TAPC's singlet state and tri-*p*-tolylamine ion pairs.[37,38] It is likely that pinholes filled with TAPC (during annealing of EML) and TmPyPB (subsequent deposition on EML) are present for charges to bypass the EML in operational PhOLEDs. Annealing of melts may also result in interlayer mixing between TAPC, with T_g at 78 °C,[30] and EML for TAPC to compete favorably for excitons with the mixed and hybrid hosts by virtue of its lower E_T value than those of the hybrid and mixed hosts. Annealing of **mCP-*S*-PhSiPh3:FIrpic** at 20 °C for up to 72 h and at 80 °C for 1 h did not depress the EQE profiles while causing driving voltages to vary somewhat erratically, as shown in Fig. 3a and b. Upon thermal annealing at 100 °C for 1 h, a considerable loss in EQE accompanied by driving voltage reduction was observed, consistent with pinholes and interlayer mixing for the interpretation of satellites in the emission spectra. The sharp decline in both EQE and driving voltage shown in Fig. 3c and d upon annealing of **mCP:SiPh4:FIrpic** at 80 and 100 °C well above its T_g at 57 °C corroborates the proposition that pinholes and interlayer mixing are responsible for similar behaviors to the hybrid host. In addition, crystallization in **mCP:SiPh4:FIrpic** may also reduce the driving voltage through improved charge transport capability.[39]

As Fig. 3c is contrasted with Fig. 3a, a higher EQE value was achieved with the pristine EML comprising **mCP:SiPh4:FIrpic** than **mCP-*S*-PhSiPh3:FIrpic**, an observation to be rationalized by comparing the charge injection barrier and transport property. To a good approximation, **mCP:SiPh4** and **mCP-*S*-PhSiPh3** should possess the same HOMO and LUMO levels[21] to render identical electron and hole injection barriers into the two EMLs both doped with 10 wt% **FIrpic**. The higher EQE

value obtained with **mCP:SiPh4:FIrpic** than **mCP-𝒮-PhSiPh3:FIrpic**, both amorphous prior to thermal annealing, could be attributed to the superior charge transport ability of the mixed host to that of the hybrid host as indicated by the *I–V* characteristics of the PhOLEDs with pristine EMLs; Fig. 3d *versus* Fig. 3b. Further comparison of EQE values between the two host systems is made difficult by crystallization of EMLs with the mixed host but not the hybrid host upon thermal annealing.

With the physical integrity of EMLs in question during thermal annealing above their T_gs, ITO/MoO_3/TAPC/EML/TmPyPB stacks were fabricated for thermal annealing at 60 °C, *i.e.* 19 °C below TmPyPB's T_g for varying durations. Annealing at 60 °C was intended for expedited thermal evaluation while accommodating the expected temperature rise in a typical operational device.[40] An independent vacuum-sublimed TmPyPB film and all layers in the stack ITO/MoO_3/TAPC/**mCP-𝒮-PhSiPh3:FIrpic**/TmPyPB remained amorphous after thermal annealing at 60 °C for 14 days and 198 h, respectively based on polarizing optical microscopy and electron diffraction (Fig. 4a and b). The polycrystalline features of EML, however, emerged upon thermal annealing at 60 °C of ITO/MoO_3/TAPC/**mCP:SiPh4:FIrpic**/TmPyPB beginning in 1 h; see Fig. 4c–e. No satellite peaks, however, were observed in the emission spectra shown in Fig. S6a and b† for amorphous and polycrystalline EMLs in hybrid and mixed hosts annealed at 60 °C, thus arguing against pinholes and interlayer mixing as with annealing at 80 or 100 °C.

A PhOLED device subjected to repeated uses over the range of current density from 0.1 to 50 mA cm^{-2} is shown in Fig. 5, which is found to be equivalent to a pristine PhOLED tested at 50 mA cm^{-2} in terms of EQE and driving voltage. According to Fig. 5a, EQE values with **mCP-𝒮-PhSiPh3:FIrpic** are by and large unaffected at 7 to 8% with annealing at 60 °C up to 24 h before decreasing monotonically with extended annealing time. Under 60 °C annealing for 96 h, the stack of ITO/MoO_3/TAPC retained its hole transport capability as demonstrated in Fig. 1a. In the absence of crystallization of any layer up to TmPyPB, pinholes and interlayer mixing at interfaces of EML with its neighboring

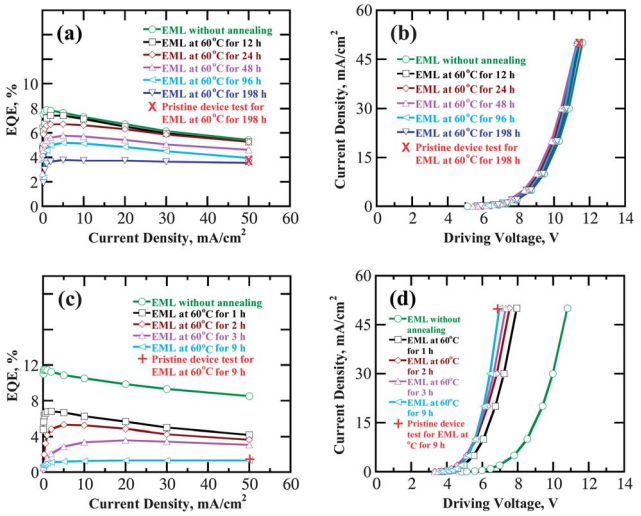

Fig. 5 (a) EQE and (b) driving voltage as functions of current density for PhOLED devices containing **mCP-𝒮-PhSiPh3:FIrpic**, and (c) EQE and (d) driving voltage as functions of current density for PhOLED devices containing **mCP:SiPh4:FIrpic** with half-devices, ITO/MoO_3/TAPC/EML/TmPyPB, annealed at 60 °C for various periods of time. Typical experimental errors for EQE and driving voltage are ±8 and ±6%, respectively. Pristine **mCP-𝒮-PhSiPh3:FIrpic** and **mCP:SiPh4:FIrpic** PhOLED devices were characterized at 50 mA cm^{-2} half-devices, ITO/MoO_3/TAPC/EML/TmPyPB, annealed at 60 °C for 198 h and 9 h indicated as × and +, respectively.

layers, one should look at BPhen/LiF/Al to identify other sources of device failure. A similar hybrid host, **SimCP**,[41] consisting of **mCP** linked to **SiPh3** without a flexible linkage afforded EQE values at 9 and 14% with **FIrN4** and **FIrpic** as blue dopants, respectively, in a different device structure than ours. Moreover, **FIrN4** at 7 wt% in a **SimCP** thin film was found to crystallize at 70 °C,[42] evidently lacking in morphological stability. In sharp contrast to **mCP-𝒮-PhSiPh3:FIrpic**, EQE values with **mCP:SiPh4:FIrpic** decrease by 40 to 80% (Fig. 5c) with about 40% reduction in driving voltage (Fig. 5d) upon annealing at

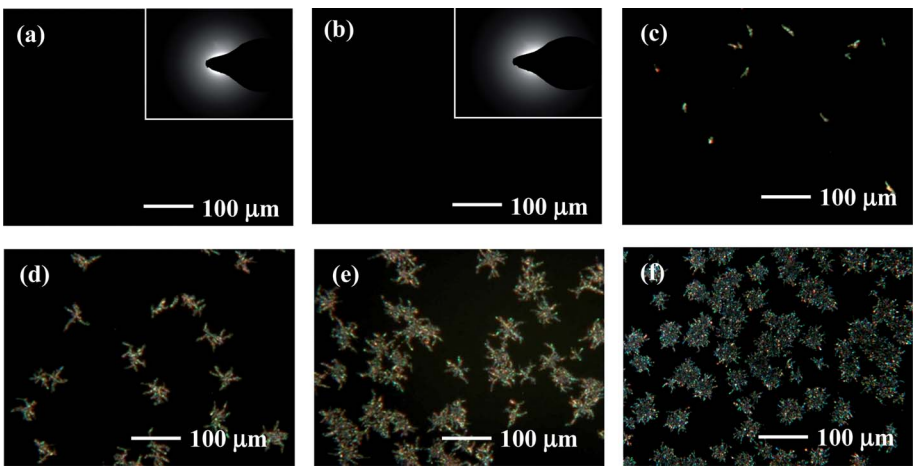

Fig. 4 Polarizing optical micrographs of (a) TmPyPB annealed at 60 °C for up to 14 days, (b) ITO/MoO_3/TAPC/**mCP-𝒮-PhSiPh3:FIrpic**/TmPyPB annealed at 60 °C for up to 198 h, and ITO/MoO_3/TAPC/**mCP:SiPh4:FIrpic**/TmPyPB annealed at 60 °C for (c) 1 h, (d) 2 h, (e) 3 h, and (f) 9 h. Insets in (a) and (b): electron diffraction images of TmPyPB and MoO_3/TAPC/**mCP-𝒮-PhSiPh3:FIrpic**/TmPyPB annealed at 60 °C for up to 14 days and 198 h, respectively.

60 °C from 1 to 3 h as a result of crystallization. Note in addition the slightly less extent of voltage reduction than that shown in Fig. 3d with annealing at 80 and 100 °C for 1 h where both crystallization and pinhole formation might have come into play.

With the reported T_g and T_m at 62 and 220 °C,[43] respectively, polycrystallinity was found to prevail in a vacuum-sublimed, amorphous BPhen film kept at 20 °C overnight, thus disabling an investigation of how thermal annealing of the PhOLED device in its entirety may affect its performance, particularly with a relatively stable EML comprising **mCP-*Ø*-PhSiPh3:FIrpic**. To improve the modest EQE values using **mCP-*Ø*-PhSiPh3**, electron and hole fluxes through EML should be balanced by mixing chemical hybrids of **mCP** and **SiPh4** at varying molar ratios while ensuring miscibility, elevated T_g, and stability against crystallization over those of equivalent physical mixtures.[44]

Experimental section

Materials

The compounds, 1,1-bis[4-[*N*,*N*-di(*p*-tolyl)aminophenyl]cyclohexane (**TAPC**, >99%, Nichem, Taiwan), 1,3,5-tri(*m*-pyrid-3-yl-phenyl)benzene (**TmPyPB**, >99%, Nichem, Taiwan), 4,7-diphenyl-[1,10]phenanthroline (**BPhen**, >99%, Nichem, Taiwan), and bis(4,6-di-fluorophenyl)-pyridinato-*N*,*C*2′)iridium(III) picolinate (**FIrpic**, >99%, Nichem, Taiwan), were used as received without further purification. Tetraphenylsilane (**SiPh4**, 95%, Alfa Aesar) was purified by sublimation before use, and its characterization data to support ultimate purity are presented in the ESI.† Synthesis, purification, and characterization data of 1,3-bis(9-carbazolyl)benzene, **mCP**, and (4-(3-(3,5-bis(9-carbazolyl)-phenyl)propyl)phenyl) triphenylsilane, **mCP-*Ø*-PhSiPh3**, are also described in the ESI.† ^{1}H NMR spectra were acquired in $CDCl_3$ with an Avance-400 spectrometer (400 MHz). Elemental analysis was carried out at the Elemental Analysis Facility, University of Rochester. Molecular weights were measured with a MALDI-TOF mass spectrometer (Brüker Autoflex III).

Thin film preparation and characterization

Thin films were prepared by thermal vacuum evaporation on fused silica substrates at 4 Å s^{-1} under 5 × 10^{-6} torr. The thickness was measured by a stylus-type profilometer (D-100, KLA Tencor). The film morphology was characterized by polarizing optical microscopy (Leitz Orthoplan-Pol) with a digital camera (MicroPix C-1024). With a transmission electron microscope (FEI Tecnai F20), electron diffraction images were collected on films mounted onto copper grids after floating off sodium chloride substrates (International Crystal Laboratories) in deionized water.

PhOLED fabrication and characterization

ITO substrates were thoroughly cleaned and treated with oxygen plasma prior to depositing a 3 nm thick MoO_3 layer by thermal vacuum evaporation at 0.3 Å s^{-1}, followed by a hole-transport layer (30 nm), TAPC, and an EML (30 nm) comprising Host : **FIrpic** at a mass ratio of 9 : 1, both at 4 Å s^{-1}. Layers of TmPyPB (10 nm), BPhen (30 nm), and LiF (1 nm) were deposited consecutively at 4 Å s^{-1}, 4 Å s^{-1}, and 0.2 Å s^{-1}, respectively. The devices were completed by deposition of aluminum (100 nm) at 10 Å s^{-1} through a shadow mask to define active areas of 0.1 cm^2 (0.32 cm × 0.32 cm) each. All evaporation processes were carried out at a base pressure less than 5 × 10^{-6} torr. Thermal annealing of ITO/MoO_3/TAPC/EML was performed at 20 °C for varying time periods and at 80 and 100 °C for 1 h each, and of ITO/MoO_3/TAPC/EML/TmPyPB at 60 °C for varying time periods in a glove box filled with nitrogen. All devices were characterized by a source-measure unit (Keithley 2400) and a spectroradiometer (PhotoResearch PR650) in the ambient environment without encapsulation. Only the front-view performance data were collected.

Summary

A mixed host, **mCP:SiPh4** at a 1 : 1 molar ratio, and its hybrid counterpart, **mCP-*Ø*-PhSiPh3**, both doped with **FIrpic** at 10 wt %, are used to elucidate how thermally activated morphological changes in the EML may affect PhOLED performance. The annealing temperature relative to EML's T_g and whether or not the EML presents a free surface during annealing are two governing parameters. Annealing of **mCP:SiPh4:FIrpic** at 20, 60, 80, and 100 °C relative to its T_g at 57 °C with and without a free surface all induced crystallization. Flanking **FIrpic's** major phosphorescence peaks at 470 and 500 nm upon annealing above T_g with a free surface, satellites at 420 and 580 nm are attributable to emission from TAPC's singlet state and tri-*p*-tolylamine ion pairs filling the pinholes in EML and interlayer mixing. Crystallization, pinhole formation, and/or interlayer mixing are responsible for the decreased EQE and driving voltage for the most part, depending on the involvement of a free surface. Annealing of **mCP:SiPh4:FIrpic** at 60 °C without a free surface presented by EML for 1 h led to about 50% loss in EQE. In contrast, annealing of **mCP-*Ø*-PhSiPh3:FIrpic** at 20, 60, and 80 °C relative to its T_g at 97 °C with and without a free surface did not cause crystallization or satellite emission. In particular, a pristine device's EQE persisted up to 24 h annealing at 60 °C without a free surface presented by EML, beyond which other sources of device failure took over. Annealing of **mCP-*Ø*-PhSiPh3:FIrpic** at 100 °C with a free surface, however, resulted in a considerable decline in both EQE and driving voltage accompanied by relatively minor satellite emission attributable to pinholes and interlayer mixing. Compared to physical mixing, the concept of chemical hybrids with a flexible linkage holds promise for long-lived PhOLED devices by elevating T_g while preventing crystallization of an amorphous EML.

Acknowledgements

The authors thank Professors Lewis J. Rothberg and Ching W. Tang, and Mr Kevin P. Klubek for their technical advice, Dr Lichang Zeng for synthesizing **mCP** in addition to helpful discussions, and Mr Millard Myman for the measurement of the triplet energy of **mCP-*Ø*-PhSiPh3**. They also thank Professor Ching W. Tang for access to the PhOLED device fabrication and characterization facilities. They are grateful for the financial support provided by the Department of Energy under Grant no. DE-EE0003296 for a solid-state lighting team project.

Additional funding was provided by the Department of Energy Office of Inertial Confinement Fusion under Cooperative Agreement no. DE-FC52-08NA28302 with Laboratory for Laser Energetics at the University of Rochester. The support of DOE does not constitute an endorsement by DOE of the views expressed in this article.

References

1 C. Ulbricht, B. Beyer, C. Friebe, A. Winter and U. S. Schubert, *Adv. Mater.*, 2009, **21**, 4418.
2 M. E. Kondakova, J. C. Deaton, T. D. Pawlik, D. J. Giesen, D. Y. Kondakov, R. H. Young, T. L. Royster, D. L. Comfort and J. D. Shore, *J. Appl. Phys.*, 2010, **107**, 014515.
3 D. Y. Kondakov, W. C. Lenhart and W. F. Nichols, *J. Appl. Phys.*, 2007, **101**, 024512.
4 F. So and D. Kondakov, *Adv. Mater.*, 2010, **22**, 3762.
5 H. Aziz and Z. D. Popovic, *Chem. Mater.*, 2004, **16**, 4522.
6 M. A. Baldo, S. Lamansky, P. E. Burrows, M. E. Thompson and S. R. Forrest, *Appl. Phys. Lett.*, 1999, **75**, 4.
7 R. J. Holmes, S. R. Forrest, Y.-J. Tung, R. C. Kwong, J. J. Brown, S. Garon and M. E. Thompson, *Appl. Phys. Lett.*, 2003, **82**, 2422.
8 M.-H. Tsai, Y.-H. Hong, C.-H. Chang, H.-C. Su, C.-C. Wu, A. Matoliukstyte, J. Simokaitiene, S. Grigalevicius, J. V. Grazulevicius and C.-P. Hsu, *Adv. Mater.*, 2007, **19**, 862.
9 P. E. Burrows, A. B. Padmaperuma, L. S. Sapochak, P. Djurovich and M. E. Thompson, *Appl. Phys. Lett.*, 2006, **88**, 183503.
10 M.-K. Leung, C.-C. Yang, J.-H. Lee, H.-H. Tsai, C.-F. Lin, C.-Y. Huang, Y. O. Su and C.-F. Chiu, *Org. Lett.*, 2007, **9**, 235.
11 H.-F. Chen, S.-J. Yang, Z.-H. Tsai, W.-Y. Hung, T.-C. Wang and K.-T. Wong, *J. Mater. Chem.*, 2009, **19**, 8112.
12 M. A. Baldo, C. Adachi and S. R. Forrest, *Phys. Rev. B: Condens. Matter*, 2000, **62**, 10967.
13 D. Song, S. Zhao, Y. Luo and H. Aziz, *Appl. Phys. Lett.*, 2010, **97**, 243304.
14 S. H. Kim, J. Jang and J. Y. Lee, *Appl. Phys. Lett.*, 2007, **91**, 083511.
15 J. Lee, J.-I. Lee, J. Y. Lee and H. Y. Chu, *Appl. Phys. Lett.*, 2009, **94**, 193305.
16 D. P.-K. Tsang, M.-Y. Chan, A. Y.-Y. Tam and V. W.-W. Yam, *Org. Electron.*, 2011, **12**, 1114.
17 Y. Tao, C. Yang and J. Qin, *Chem. Soc. Rev.*, 2011, **40**, 2943.
18 A. Chaskar, H.-F. Chen and K.-T. Wong, *Adv. Mater.*, 2011, **23**, 3876.
19 S. Liu, F. He, H. Wang, H. Xu, C. Wang, F. Li and Y. Ma, *J. Mater. Chem.*, 2008, **18**, 4802.
20 C.-C. Lee, S.-W. Liu and Y.-T. Chung, *J. Phys. D: Appl. Phys.*, 2010, **43**, 075102.
21 L. Zeng, T. Y.-H. Lee, P. B. Merkel and S. H. Chen, *J. Mater. Chem.*, 2009, **19**, 8772.
22 K. Brunner, A. van Dijken, H. Börner, J. J. A. M. Bastiaansen, N. M. M. Kiggen and B. M. W. Langeveld, *J. Am. Chem. Soc.*, 2004, **126**, 6035.
23 L. Xiao, Z. Chen, B. Qu, J. Luo, S. Kong, Q. Gong and J. Kido, *Adv. Mater.*, 2011, **23**, 926.
24 J. Lee, J.-I. Lee, J.-W. Lee and H. Y. Chu, *Org. Electron.*, 2010, **11**, 1159.
25 R. J. Holmes, B. W. D'Andrade, S. R. Forrest, X. Ren, J. Li and M. E. Thompson, *Appl. Phys. Lett.*, 2003, **83**, 3818.
26 T. Motoyama, H. Sasabe, Y. Seino, J.-I. Takamatsu and J. Kido, *Chem. Lett.*, 2011, 306.
27 X. Gu, H. Zhang, T. Fei, B. Yang, H. Xu, Y. Ma and X. Liu, *J. Phys. Chem. A*, 2010, **114**, 965.
28 C. Adachi, R. C. Kwong, P. Djurovich, V. Adamovich, M. A. Baldo, M. E. Thompson and S. R. Forrest, *Appl. Phys. Lett.*, 2001, **79**, 2082.
29 I. B. Johns, E. A. McElhill and J. O. Smith, *J. Chem. Eng. Data*, 1962, **7**, 277.
30 K. Naito and A. Miura, *J. Phys. Chem.*, 1993, **97**, 6240.
31 S. H. Chen, H. Shi, B. M. Conger, J. C. Mastrangelo and T. Tsutsui, *Adv. Mater.*, 1996, **8**, 998.
32 B. C. Edwards and P. J. Phillips, *Polymer*, 1974, **15**, 351.
33 M. G. Mason, C. W. Tang, L.-S. Hung, P. Raychaudhuri, J. Madathil, D. J. Giesen, L. Yan, Q. T. Le, Y. Gao, S.-T. Lee, L. S. Liao, L. F. Cheng, W. R. Salaneck, D. A. dos Santos and J. L. Brédas, *J. Appl. Phys.*, 2001, **89**, 2756.
34 S.-J. Su, Y. Takahashi, T. Chiba, T. Takeda and J. Kido, *Adv. Funct. Mater.*, 2009, **19**, 1260.
35 K. Goushi, R. Kwong, J. J. Brown, H. Sasabe and C. Adachi, *J. Appl. Phys.*, 2004, **95**, 7798.
36 K. W. Andrews, D. J. Dyson and S. R. Keown, in *Interpretation of Electron Diffraction Patterns*, Plenum Press, New York, 1967, pp. 14–27.
37 J. Kalinowski, G. Giro, M. Cocchi, V. Fattori and P. Di Macro, *Appl. Phys. Lett.*, 2000, **76**, 2352.
38 T.-Y. Kim and D.-G. Moon, *Trans. Electr. Electron. Mater.*, 2011, **12**, 83.
39 A. R. Aiyar, J.-I. Hong, R. Nambiar, D. M. Collard and E. Reichmanis, *Adv. Funct. Mater.*, 2011, **21**, 2652.
40 X. Zhou, J. He, L. S. Liao, M. Lu, X. M. Ding, X. Y. Hou, X. M. Zhang, X. Q. He and S. T. Lee, *Adv. Mater.*, 2000, **12**, 265.
41 S.-J. Yeh, M.-F. Wu, C.-T. Chen, Y.-H. Song, Y. Chi, M.-H. Ho, S.-F. Hsu and C. H. Chen, *Adv. Mater.*, 2005, **17**, 285.
42 M.-F. Wu, S.-J. Yeh, C.-T. Chen, H. Murayama, T. Tsuboi, W.-S. Li, I. Chao, S.-W. Liu and J.-K. Wang, *Adv. Funct. Mater.*, 2007, **17**, 1887.
43 P. Kathirgamanathan, S. Surendrakumar, S. Ravichandran, R. R. Vanga, J. Antipan-Lara, S. Ganeshamurugan, M. Kumaravel, G. Paramaswara and V. Arkley, *Chem. Lett.*, 2010, **39**, 1222.
44 H. Shi and S. H. Chen, *Liq. Cryst.*, 1995, **18**, 733.

